Synthesis and Luminescence Properties of a Nonsymmetrical Ligand-Bridged $Re^{I}-Re^{I}$ Chromophore

W.-M. Xue, N. Goswami, David M. Eichhorn,* Peter L. Orizondo, and D. Paul Rillema*

Department of Chemistry, Wichita State University, Wichita, Kansas 67260-0051

Received February 8, 2000

The preparation and the physical and photophysical properties of three complexes containing the bridging ligand 5-(2-(4-pyridyl)ethyl)-2-(2-pyridyl)pyrimidine (pypm-py) are described. Two of the complexes are monometallic, $[Re(pypm\text{-}py)(py)(CO)_3]^+$ and $[Re(phen)(py\text{-}pypm)(CO)_3]^+$, and one is bimetallic, $[(CO)_3(py)Re(pypm\text{-}py)Re(phen)(CO)_3]^{2+}$, where phen is 1,10-phenanthroline and py is pyridine. $[Re(pypm\text{-}py)(py)(CO)_3](CF_3SO_3)$ crystallized in the space group $P2_1/n$ with $a = 13.98$ (1) Å, $b = 12.704$ (6) Å, $c = 15.66$ (1) Å, and $Z = 4$. The Re−N(pypm) bond distances for Re−N(py of pypm) = 2.167(9) Å and for Re−N(pm of pypm) = 2.202 (9) Å. The Re−N(py) bond distance is 2.203(9) Å. The complexes exhibit CO infrared-active bands in the 1900−2100 cm^{-1} region of the infrared spectrum; three bands were present for $[Re(pypm\text{-}py)(py)(CO)_3]^+$, but only two for the other complexes. Methylene protons for $[Re(pypm\text{-}py)(py)(CO)_3]^+$ are nonequivalent on the basis of NMR spectra analysis, but are equivalent for the other two complexes. Oxidation of the complexes occurs in the 1.83−1.87 V vs SSCE region and is attributed to the $Re^{2+/+}$ redox couple; three to four reductions occur, the first of which is assigned to reduction of the coordinated diimine ligand, either the ($pypm^{0/-}$-py) or the ($phen^{0/-}$) couple occurring at ∼ −1.05 and ∼ −1.23 V, respectively. The three complexes undergo electronic excitation in the 300−400 nm region assigned to $d\pi \rightarrow \pi^*$(diimine) transitions and in the 200−300 nm region assigned to intraligand $\pi \rightarrow \pi^*$ transitions. Strong emission occurs from the complexes in solution at room temperature. The emission bands are structureless, and the positions are solvent dependent, consistent with MLCT emitters. Quantum efficiencies and emission lifetimes in 4:1 ethanol/methanol at room temperature fall in the order $[Re(phen)(py\text{-}pypm)(CO)_3]^+$ ($\phi_{em} = 0.087$, $\tau = 1.65$ μs) > $[(CO)_3(py)Re(pypm\text{-}py)Re(phen)(CO)_3]^{2+}$ ($\phi_{em} = 0.037$, $\tau = 1.09$ μs) > $[Re(pypm\text{-}py)(py)(CO)_3]^+$ ($\phi_{em} = 0.014$, $\tau = 0.11$ μs), indicating that energy transfer occurs between the Re(phen) chromophore and the Re(pypm) center in the bimetallic complex.

Introduction

Rhenium(I) tricarbonyl complexes containing bidentate heterocyclic ligands have been a source of much interest largely due to their potential for use in solar energy conversion.[1−14] These complexes are ideally suited for such applications, as they display intense luminescence in the visible region of the spectrum and are stable to photodecomposition. In solution, emission from these complexes typically occurs from metal-to-ligand charge transfer (MLCT) states as typified by a broad, structureless emission band, which is sensitive to changes in the nature of the environment, such as temperature, solvent, and pH. At low temperature, however, and in the solid state, there is evidence for ligand-centered emission as well as MLCT emission in complexes containing phenanthroline ligands.[14a]

In this report we extend the study to an understanding of the photophysical properties of bimetallic rhenium(I) diimine

(1) (a) Geoffroy, G. L.; Wrighton, M. S. *Organometallic Photochemistry*; Academic Press: New York, 1979. (b) Lees, A. J. *Chem. Rev.* **1987**, *87*, 711.
(2) Kalyanasundaram, K. *Photochemistry of Polypyridyl and Porphyrin Complexes*; Academic Press: New York, 1992.
(3) (a) Meyer, T. J. Pure *Appl. Chem.* **1986**, *58*, 1193. (b) Tapolsky, G.; Duesing, R.; Meyer, T. J. *J. Phys. Chem.* **1989**, *93*, 2885. (c) Tapolsky, G.; Duesing, R.; Meyer, T. J. *Inorg. Chem.* **1990**, *29*, 2285. (d) Chen, P.; Curry, M.; Meyer, T. J. *Inorg. Chem.* **1989**, *28*, 2271.
(4) (a) Wrighton, M. S.; Morse, D. L. *J. Am. Chem. Soc.* **1974**, *96*, 998. (b) Giordano, P. J.; Fredericks, S. M.; Wrighton, M. S.; Morse, D. L. *J. Am. Chem. Soc.* **1978**, *100*, 2257. (c) Giordano, P. J.; Wrighton, M. S. *J. Am. Chem. Soc.* **1979**, *101*, 2888. (d) Fredericks, S. M.; Luong, J. C.; Wrighton, M. S. *J. Am. Chem. Soc.* **1979**, *101*, 7415. (e) Smothers, W. K.; Wrighton, M. S. *J. Am. Chem. Soc.* **1983**, *105*, 1067.
(5) (a) Sacksteder, L.; Zipp, A. P.; Brown, E. A.; Streich, J.; Demas, J. N.; DeGraff, B. A. *Inorg. Chem.* **1990**, *29*, 4335. (b) Leasure, R. M.; Sacksteder, L.; Nesselrodt, D.; Reitz, G. A.; Demas, J. N.; DeGraff, B. A. *Inorg. Chem.* **1991**, *30*, 3722.
(6) Vogler, A.; Kisslinger, J. *Inorg. Chim. Acta* **1986**, *115*, 193.
(7) Zipp, A. P. *Coord. Chem. Rev.* **1988**, *84*, 47.
(8) Juris, A.; Campagna, S.; Bidd, I.; Lehn, J. M.; Zeissel, R. *Inorg. Chem.* **1988**, *27*, 4007.
(9) Ruminski, R.; Cambron, R. *Inorg. Chem.* **1990**, *29*, 1574.
(10) (a) Lin, R.; Fu, Y.; Brock, C. P.; Guarr, T. F. *Inorg. Chem.* **1992**, *31*, 4346. (b) Lin, R.; Guarr, T. F. *Inorg. Chim. Acta* **1990**, *167*, 149. (c) Lin, R.; Guarr, T. F.; Duesing, R.; Meyer, T. J. *Inorg. Chem.* **1990**, *29*, 4169.
(11) Baiano, J. A.; Carlson, D. L.; Wolosh, G. M.; DeJesus, D. E.; Knowles, C. F.; Szabo, E. G.; Murphy, W. R., Jr. *Inorg. Chem.* **1990**, *29*, 2327.
(12) (a) Hino, J. K.; Della Ciana, L.; Dressick, W. J.; Sullivan, B. P. *Inorg. Chem.* **1992**, *31*, 1072. (b) Shen, Y.; Sullivan, B. P. *Inorg. Chem.* **1995**, 34, 6235. (c) Woessner, S.; Helms, J.; Houlis, J.; Sullivan, B. P. *Inorg. Chem.* **1999**, *38*, 4380.
(13) (a) Yam, V. W.-W.; Wang, K. Z.; Wang, C. R.; Yu, Y.; Cheung, K. K. *Organometallics* **1998**, *17*, 2440. (b) Yam, V. W.-W.; Chong, S. H.-F.; Cheung, K. K. *Chem. Commun. (Cambridge)* **1998**, 2121. (c) Yam, V. W.-W.; Wong, K. M.-C.; Cheung, K. K. *Organometallics* **1997**, *16*, 1740. (d) Yam, V. W.-W.; Lau, V. C.-Y.; Cheung, K. K. *Organometallics* **1996**, *15*, 1740. (e) Yam, V. W.-W.; Lau, V. C.-Y.; Cheung, K.-K. *J. Chem. Soc., Chem. Commun.* **1995**, 259.
(14) (a) Wallace, L.; Rillema, D. P. *Inorg. Chem.* **1993**, *32*, 3836. (b) Shaver, R. J.; Rillema, D. P. *Inorg. Chem.* **1992**, *31*, 4104. (c) Van Wallendael, S.; Rillema, D. P. *Coord. Chem. Rev.* **1991**, *111*, 297. (d) Van Wallendael, S.; Shaver, R. J.; Rillema, D. P.; Yoblinski, B. J.; Stathsis, M.; Guarr, T. F. *Inorg. Chem.* **1990**, *29*, 1761. (e) Sahai, R.; Rillema, D. P.; Shaver, R. J.; Van Wallendael, S.; Jackman, D. C.; Boldaji, M. *Inorg. Chem.* **1989**, *28*, 1022.

10.1021/ic000134d CCC: $19.00
Published on Web 09/15/2000

complexes. Homobimetallic heterocyclic ligand complexes of rhenium(I) have been reported with bridging ligands, such as pyrazine.[10a] These complexes exhibited substantial red shifts in luminescence energy maxima upon formation of the bimetallic complex as well as marked decreases in emission lifetimes. In our earlier work,[14c] we have examined the excited-state properties of the bimetallic complex, $[(bpy)_2Ru(bb)Re(CO)_3py]^{3+}$, where bb is 1,2-bis(4′-methyl-2,2′-bipyridyl-4-yl)ethane, bpy is 2,2′-bipyridine, and py is pyridine, and found emission from the "$(bpy)Ru(bb)^{2+}$" unit upon excitation at 355 nm, which was attributed to energy transfer from "$(bb)Re(CO)_3py^{+*}$" to "$(bpy)_2Ru(bb)^{2+}$". A comparison of the emission lifetime (τ) and quantum yield (ϕ_{em}) of $(phen)Re(CO)py^+$ ($\tau = 1.6$ μs, $\phi_{em} = 0.180$, CH_3CN, 298 K) to those of $(bpy)Re(CO)_3py^+$ ($\tau = 0.66$ μs, $\phi_{em} = 0.059$, CH_3CN, 298 K) revealed that the energy transfer process could potentially be enhanced for similar bimetallic complexes based on 1,10-phenanthroline (phen) complexes.[5a] Our interest in this report is in the photophysical behavior of a nonsymmetric bimetallic complex of rhenium(I) based on a new bridging ligand pypm-py, 5-(2-(4-pyridyl)-ethyl)-2-(2-pyridyl)pyrimidine, where py has been coordinated to "$Re(phen)(CO)_3^+$" and pypm to "$Re(CO)_3py^+$". Large red shifts in emission were not expected to occur upon dimer formation because the bridge contains an ethylene group inhibiting communication,[13e] but not energy transfer between the metal centers.

Experimental Section

Materials. $[Re(phen)(CO)_4](CF_3SO_3)$[14b] and 2-(pyridyl)amidine hydrochloride (II)[15] were prepared by literature methods. Rhenium pentacarbonyl chloride (Pressure Chemical Co.), silver trifluoromethanesulfonate (Aldrich), 1,10-phenanthroline (GFS), 2-vinylpyridine (Aldrich), palladium on charcoal (K & K Laboratories, Inc.), sodium acetate (Fisher) and phosphorus oxychloride (Aldrich) were used as purchased. Commercially purchased tetrabutylammonium hexafluorophosphate (TBAH) was of electrometric grade (Southwestern Analytical, Inc.) and was used without further purification. All solvents were purchased commercially as HPLC grade and were used without further purification. All preparations for the rhenium complexes were performed under an argon atmosphere.

Preparation of 4-(2-Pyridyl)ethylmalonate (I). 4-(2-Pyridyl)-ethylmalonate was prepared by a modification of the procedure for the preparation of 2-(2-pyridyl)ethylmalonate.[16] (4-Vinylpyridine was used in place of 2-vinylpyridine.) The reaction time was 24 h. The product was purified by column chromatography using silica gel (100−200 mesh) with ethyl acetate/petroleum ether (40−60 °C) (1:1) as the eluent. The first colorless band was collected. The product was obtained as a colorless oil after the solvent was evaporated using a rotary evaporator. Yield: 43%. ^{1}H NMR ($CDCl_3$) δ (ppm): 1.28 (m, 6H, CH_3), 2.23 (m, 2H, CH_2−CH), 2.67 (m, 2H, CH_2-py), 3.33 (m, 1H, CH), 4.21 (m, 4H, CH_2−CH_3), 7.13 (m, 2H, py-H), 8.51 (m, 2H, py-H).

Preparation of 4,6-Dihydroxy-5-(2-(4-pyridyl)ethyl)-2-(2-pyridyl)-pyrimidine (III). 4,6-Dihydroxy-5-(2-(4-pyridyl)ethyl)-2-(2-pyridyl)-pyrimidine was prepared by a modification of the procedure used to prepare 4,6-dihydroxy-2-(2-pyridyl)pyrimidines.[17] Sodium metal (5 g) was dissolved in 350 mL of absolute ethanol; then 2-(pyridyl)amidine hydrochloride (**II**, 5.0 g, 34.8 mmol) was added. After the mixture was stirred at room temperature for $^1/_2$ h, 4-(2-pyridyl)ethylmalonate (**I**, 9.2 g, 34.8 mmol) was added. The mixture was refluxed for 20 h. White solid was removed by filtration, and then the solvent was removed from the filtrate by rotary evaporation. The residue was dissolved in 400 mL of water, the solution was neutralized with aqueous 6 M HCl, and the crude product precipitated. A white product was collected upon recrystallization of the crude product from absolute C_2H_5OH. Yield: 3.7 g (36%). Mp: 266.6−268.0 °C. ^{1}H NMR (d_6-DMSO) δ (ppm): 2.64 (m, 2H, CH_2), 2.76 (m, 2H, CH_2), 7.21 (dd, 2H), 7.60 (m, 1H), 8.01 (td, 1H), 8.22 (dt, 1H), 8.38 (dd, 2H), 8.69 (m, 1H).

Preparation of 4,6-Dichloro-5-(2-(4-pyridyl)ethyl)-2-(2-pyridyl)-pyrimidine (IV). 4,6-Dichloro-5-(2-(4-pyridyl)ethyl)-2-(2-pyridyl)-pyrimidine was prepared using the procedure reported for preparing 4,6-dichloro-2-(2-pyridyl)pyrimidines.[17] The method involved heating one part by weight of 4,6-dihydroxy-5-(2-(4-pyridyl)ethyl)-2-(2-pyridyl)pyrimidine (**III**) in 10 parts by weight of phosphorus oxychloride. The product was recrystallized from $CH_2Cl_2/(C_2H_5)_2O$. Yield: 74%. Mp: 167.0 °C dec. ^{1}H NMR ($CDCl_3$) δ (ppm): 2.96 (m, 2H, CH_2), 3.27 (m, 2H, CH_2), 7.20 (dd, 2H), 7.46 (m, 1H), 7.89 (td, 1H), 8.48 (m, 1H), 8.56 (m, 2H), 8.88 (m, 1H).

Preparation of 5-(2-(4-pyridyl)ethyl)-2-(2-pyridyl)pyrimidine (pypm-py). 5-(2-(4-Pyridyl)ethyl)-2-(2-pyridyl)pyrimidine was obtained by the catalytic dehalogenation of 4,6-dichloro-5-(2-(4-pyridyl)ethyl)-2-(2-pyridyl)pyrimidine (**IV**) over palladium on carbon (5%) in ethanolic solution containing sufficient sodium acetate to neutralize the liberated hydrogen chloride.[17] The initial hydrogen pressure was 40 psi, and the reaction was allowed to continue for 2 days. The mixture was filtered, the solvent was removed with a rotary evaporator, and the residue was extracted with benzene. The extract was dried over magnesium sulfate and filtered, and the filtrate was concentrated. Petroleum ether (40−60 °C) was added to precipitate the product. Yield: 24%. Mp: 114.0−115.0 °C. Anal. Calcd for $C_{16}H_{14}N_4$: C, 73.26; H, 5.38; N, 21.36. Found: C, 73.46; H, 5.45; N, 21.14. ^{1}H NMR ($CDCl_3$) δ (ppm): 2.99 (m, 4H, CH_2), 7.07 (dd, 2H), 7.37 (m, 1H), 7.83 (td, 1H), 8.44 (dt, 1H), 8.49 (dd, 2H), 8.65 (s, 2H), 8.80 (m, 1H). ^{13}C NMR ($CDCl_3$): 30.9(CH_2), 36.1(CH_2), 123.3, 123.8, 124.9, 132.5, 137.0, 148.8, 150.0, 150.1, 154.5, 157.5, 162.1.

Preparation of [Re(pypm-py)(py)(CO)$_3$](CF$_3$SO$_3$). $[Re(pypm\text{-}py)(py)(CO)_3](CF_3SO_3)$ was prepared by a method similar to that for the preparation of $[Re(L\text{-}L)(CO)_3(py)](CF_3SO_3)$, where L-L are substituted phenanthroline ligands.[14a] $Re(CO)_5Cl$ (0.50 g, 1.38 mmol) was dissolved in 80 mL of methylene chloride. Silver trifluoromethane sulfonate (0.37 g, 1.45 mmol) was added to the solution containing the rhenium complex. The mixture was stirred at room temperature in the dark for 18 h. The AgCl precipitate, which formed, was removed by filtration and was washed with 20 mL of methylene chloride. The solvent was removed from the filtrate using a rotary evaporator, the residue was dissolved in 25 mL of methanol, and the solution was heated at reflux for 1 h. Pypm-py (0.40 g, 1.5 mmol) in 25 mL of methanol was then added dropwise to the cooled reaction solution. The mixture was refluxed for another 16 h. The solvent was then removed using a rotary evaporator, and pyridine (20 mL) was added to the residue. The resulting yellow solution was heated at reflux for 18 h, after which time the pyridine was removed using a rotary evaporator. The remaining solids were dissolved in CH_2Cl_2 (ca. 5 mL) and purified by column chromatography on neutral alumina (60−325 mesh; column dimensions 15 × 1.5 cm) using CH_2Cl_2/CH_3CN (1:1) as the eluent. A yellow band was collected. The solvent was removed by rotary evaporation, and the solid product was recrystallized by diffusion of diethyl ether into an acetonitrile solution. Yield: 0.70 g (67%). Anal. Calcd for $C_{25}H_{19}N_5O_6F_3SRe$: C, 39.42; H, 2.52; N, 9.20. Found: C, 39.21; H, 2.75; N, 8.98. MS (positive FAB): m/z 611 (M^+). IR: 2036, 1937, 1918 ($\nu_{C\equiv O}$). ^{1}H NMR ($CDCl_3$) δ (ppm): 3.14 (m, 4H, CH_2), 3.28 (m, 2H, CH_2), 3.42 (m, 2H, CH_2), 7.20 (dd, 4H), 7.42 (m, 4H), 7.76 (tt, 2H), 7.86 (m, 2H), 8.22−8.29 (m, 6H), 8.48 (dd, 4H), 8.66 (d, 2H), 8.95 (d, 2H), 9.00 (d, 2H), 9.07 (d, 2H).

Preparation of [Re(phen)(py-pypm)(CO)$_3$](CF$_3$SO$_3$). $[Re(phen)(CO)_4](CF_3SO_3)$ (0.20 g, 0.32 mmol) was dissolved in a solution containing 30 mL of tetrahydrofuran and 10 mL of acetone. Pypm-py (0.092 g, 0.35 mmol) in 5 mL of tetrahydrofuran was added dropwise. The mixture was refluxed for 16 h. After the solution was cooled to room temperature, it was concentrated to ca. 10 mL using a rotary evaporator. Diethyl ether was added to precipitate the product, which was purified by recrystallization from acetonitrile/diethyl ether. Yield: 80 mg (29%). Anal. Calcd for $C_{32}H_{22}N_6O_6F_3SRe$: C, 44.54; H, 2.57; N, 9.75. Found: C, 44.68; H, 2.76; N, 9.56. MS (positive FAB): m/z 713 (M^+). IR: 2027, 1927 ($\nu_{C\equiv O}$). ^{1}H NMR (CD_3COCD_3) δ (ppm): 2.92 (m, 2H, CH_2), 2.99 (m, 2H, CH_2), 7.26 (d, 2H), 7.50 (m, 1H),

(15) Schaefer, F. C.; Peters, G. A. *J. Org. Chem.* **1961**, 26, 412.
(16) Doering, W. E.; Well, R. A. N. *J. Am. Chem. Soc.* **1947**, *69*, 2461.
(17) Lafferty, J. J.; Case, F. H. *J. Org. Chem.* **1967**, *32*, 1591.

7.96 (m, 1H), 8.34 (m, 5H), 8.47 (m, 4H), 8.78 (dd, 1H), 9.10 (dd, 2H), 9.89 (dd, 2H).

Preparation of $[(CO)_3(py)Re(pypm\text{-}py)Re(phen)(CO)_3](CF_3SO_3)_2$. $[Re(phen)(CO)_4](CF_3SO_3)$ (0.10 g, 0.16 mmol) was dissolved in a solution containing 30 mL of tetrahydrofuran and 10 mL of acetone. $[Re(pypm\text{-}py)(py)(CO)_3](CF_3SO_3)$ (0.12 g, 0.16 mmol) which previously had been dissolved in a solution containing 5 mL of tetrahydrofuran and 5 mL of acetone was added dropwise. The mixture was refluxed for 16 h. The volume of solution was reduced to ca. 10 mL, and diethyl ether was added to precipitate the product, which was then purified by diffusion of diethyl ether into an acetonitrile solution of the complex. Yield: 60 mg (28%). Anal. Calcd for $C_{41}H_{27}N_7O_{12}F_6S_2Re_2$: C, 36.20; H, 2.00; N, 7.21. Found: C, 35.98; H, 1.97; N, 7.24. MS (positive FAB): m/z 1212 ($M^+ + CF_3SO_3^-$). IR: 2034, 1921 ($\nu_{C\equiv O}$). ^1H NMR (CD_3COCD_3) δ (ppm): 3.24 (m, 4H, CH_2), 7.45 (m, 2H), 7.52 (t, 1H), 7.99 (m, 1H), 8.10 (m, 2H), 8.37 (m, 3H), 8.56 (m, 4H), 8.74 (t, 2H), 9.09−9.24 (m, 3H), 9.45 (dd, 2H), 9.57 (d, 1H), 9.92 (m, 2H).

Physical Measurements. IR spectra were obtained in KBr pellets with a Mattson Cynus 25 FT-IR spectrophotometer. ^1H and ^{13}C NMR spectra were obtained with a Varian Inova 400 FT-NMR spectrometer. M-H-W Laboratories, Phoenix, AZ, determined elemental analyses. The Mass Spectroscopy Laboratory at the University of Kansas determined mass spectra. UV−visible spectra were obtained with a Hewlett-Packard 8452A diode array spectrophotometer. Cyclic voltammograms were obtained with an EG&G PAR 263A potentiostat/galvanostat. The measurements were made using a platinum disk working electrode, a platinum gauze counter electrode, and a $Ag/AgNO_3$ (0.1 M in acetonitrile) reference electrode and were recorded with an IBM 325T computer. The supporting electrolyte was 0.1 M TBAH. Ferrocene was added as an internal standard. All samples were purged with argon prior to measurement. Emission spectra were obtained with a SPEX Fluorolog 212 spectrofluorimeter. All emission spectra were corrected for instrument response. Absolute emission quantum yields were measured by the method of Demas and Crosby[18] using quinine sulfate in 0.1 N sulfuric acid as the standard with a known emission quantum yield of 0.546 ($\lambda_{ex} = 355$ nm). Samples and standard solutions were thoroughly degassed with no fewer than three freeze−pump−thaw cycles before measurement. The emission quantum yields of the samples were determined according to eq 1, where the subscripts s and r refer

$$\phi_s = \phi_r(B_r/B_s)(n_s/n_r)^2(D_s/D_r) \quad (1)$$

tothe sample and the standard reference solution, respectively; n is the refractive index of the solvents; D is the integrated emission intensity; and ϕ is the luminescence quantum yield. The quantity B is calculated by $B = 1 - 10^{-AL}$, where A is the absorbance at the excitation wavelength and L is the optical path length. Excited-state lifetimes were determined by exciting the samples at 355 nm using an OPOTEK optical parametric oscillator pumped by a frequency-tripled Nd:YAG laser (Continuum Surlite, run at ≤1.5 mJ/10 ns pulse). Spectral regions were isolated using a Hamamatsu R955 PMT in a cooled housing (−15 °C, Amherst) coupled to an Acton SpectraPro 275 monochromator.

X-ray Crystallography. The data were collected for the structure of $[Re(pypm\text{-}py)(py)(CO)_3](CF_3SO_3)$ using graphite-monochromated Mo Kα radiation on an Enraf-Nonius CAD4 diffractometer controlled by software running on a SGI O2 computer. A yellow crystal was affixed to the tip of a glass fiber with Paratone-N oil (Exxon) and then transferred to the cold stream of the diffractometer operating at −110 °C. The unit cell was determined from the setting angles of 24 reflections with $20° < 2\theta < 23°$ and confirmed by axial photographs; 3933 reflections were collected ($\omega-2\theta$; $+h, +k, \pm l$; $2° < 2\theta < 45°$) giving a unique set of 3787 reflections ($R_{int} = 0.034$) and 2926 observed reflections ($I > 2\sigma(I)$). The data were processed and the structure was solved and refined using the TeXsan package.[19] The data were corrected for Lorentz and polarization effects and secondary extinction (6.687×10^{-8}), and an empirical absorption correction was applied using the DIFABS program.[20] No decay was detected by measurement of three intense reflections. The structure was solved by direct methods[21] and refined by full-matrix least-squares techniques with values for $\Delta f'$ and $\Delta f''$ from Creagh and McAuley.[22] The highest and lowest peaks in the final difference Fourier map were located in the vicinity of the Re atom. All non-hydrogen atoms were refined with anisotropic temperature factors. Hydrogen atoms were included at idealized positions, but were not refined. Pertinent details are given in Table 1.

Table 1. Crystallographic Data

formula	$ReC_{25}H_{19}N_5O_6SF_3 \cdot H_2O$	V, Å^3	2724(3)
fw (g/mol)	776.72	Z	4
cryst dimens	0.20 × 0.20 × 0.50 mm	ρ_{calc}, g/cm^3	1.894
cryst syst	monoclinic	T, °C	−110
space group	$P2_1/n$	μ(Mo Kα), cm^{-1}	46.15
cryst color	yellow	λ, Å	0.71069
a, Å	13.98(1)	R^a ($I > 2\sigma(I)$)	0.037
b, Å	12.704(6)	$R_w{}^b$ ($I > 2\sigma(I)$)	0.059
c, Å	15.66(1)	gof	2.30
β, deg	101.72(7)		

$^a R = \sum||F_o| - |F_c||/\sum|F_o|$. $^b R_w = [\sum w(|F_o| - |F_c|)^2/wF_o^2]^{1/2}$.

Results and Discussion

Preparation of Compounds. The synthetic route for preparing the pypm-py ligand is shown in Scheme 1. It consisted of four basic steps. Vinylpyridine was first added to the deprotonated methylene group of 2,4-pentanedione yielding product **I**, **I** then was reacted with 2-(pyridyl)amidine (**II**) to yield the dihydroxy pypm-py derivative (**III**), **III** was then converted into the dichoride (**IV**) by reaction with $POCl_3$, and then the chloride groups were replaced with hydrogen atoms to yield pypm-py by catalytic reduction of **IV** in the presence of hydrogen gas.

The syntheses of $[Re(pypm\text{-}py)(py)(CO)_3]CF_3SO_3$, $[Re(phen)(py\text{-}pypm)(CO)_3]CF_3SO_3$, and $[(CO)_3(py)Re(pypm\text{-}py)Re(phen)(CO)_3](CF_3SO_3)_2$ are outlined in Scheme 2. The basic intermediate was the reactive Re(I) pentacarbonyl trifluoromethanesulfonate complex. It was then reacted with 1,10-phenanthroline and pypm-py to yield the diimine tetracarbonyl derivatives, which added either neat pyridine to yield the monometallic complexes or the uncoordinated pyridine of coordinated pypm-py to yield the bimetallic derivative.

The NMR spectrum for the methylene protons of $[Re(pypm\text{-}py)(py)(CO)_3]^+$ as shown in Figure 1 consisted of three signals which integrated as 1:1:2. These signals are interpreted to arise from nonequivalent methylene groups, one neighboring the uncoordinated pyridine ring and the other neighboring the coordinated pyrimidine unit. The methylene group neighboring the pyrimidine ring contains two nonequivalent protons, which give rise to the two signals integrating as one proton each. However, no evidence for nonequivalent methylene protons was found in the ^1H NMR spectrum of $[(CO)_3(py)Re(pypm\text{-}py)Re(phen)(CO)_3]^{2+}$ after the uncoordinated pyridine unit was coordinated to the "$Re(phen)(CO)_3$" unit.

$[Re(pypm\text{-}py)(py)(CO)_3]^+$ displayed three carbonyl stretching bands with the highest energy transition appearing as a very sharp peak at 2036 cm^{-1}. The two remaining bands at 1937 and 1918 cm^{-1} were relatively broad and overlap considerably. Two CO stretching bands were observed for $[Re(phen)(py\text{-}pypm)(CO)_3]^+$ and $[(CO)_3(py)Re(pypm\text{-}py)Re(phen)(CO)_3]^{2+}$: a high-energy transition at 2027 cm^{-1} in the former and at 2034

(18) Demas, J. N.; Crosby, G. A. *J. Phys. Chem.* **1971**, *75*, 991.
(19) TeXsan: *Crystal Structure Analysis Package*; Molecular Structure Corporation: The Woodlands, Texas, 1985 and 1992.
(20) DIFABS: Walker, N.; Stuart, D. *Acta Crystallogr.* **1983**, *A39*, 158.
(21) SIR92: Altomare, A.; Cascarano, M.; Giacorazzo, C.; Guagliardi, A. *J. Appl. Crystallogr.* **1993**, *26*, 343.
(22) Creagh, D. C.; McAuley, W. J. In *International Tables for Crystallography*; Wilson, A. J., Ed.; Kluwer Academic Publishers: Boston, 1992; Vol. C, Tables 4.2.6.8, pp 219−222.

Scheme 1. Synthetic Route for Preparing Pypm-py

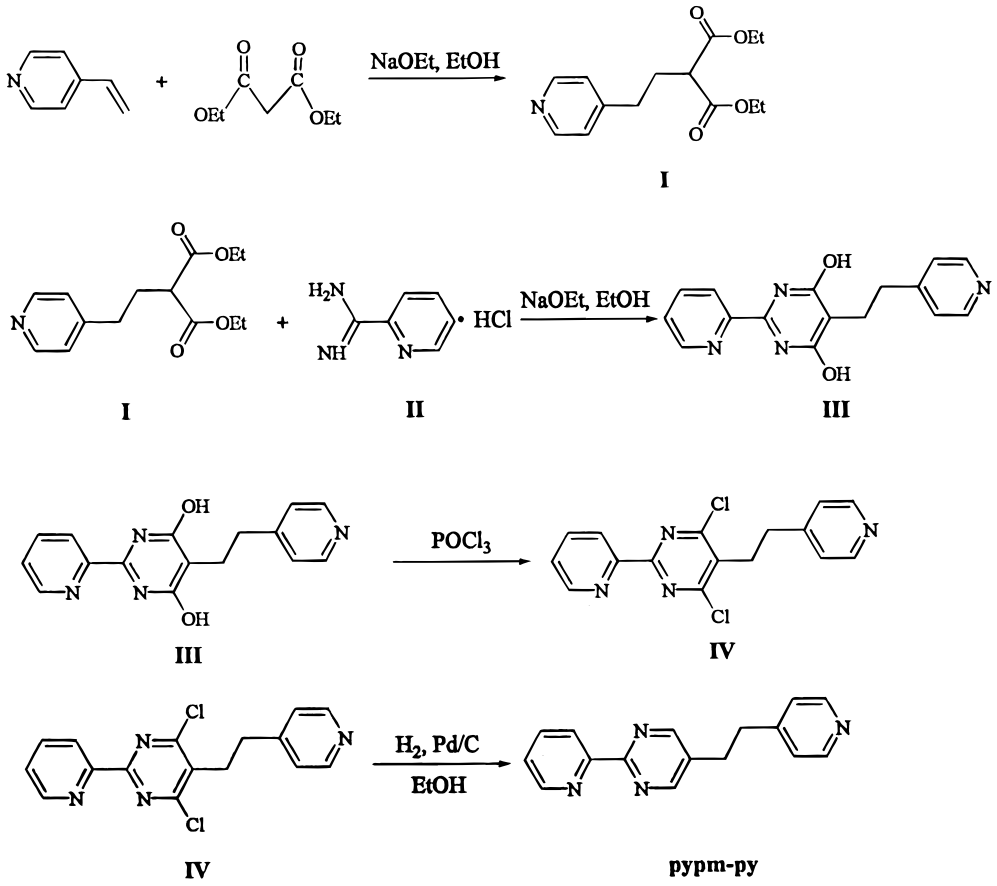

cm^{-1} in the latter; a low-energy, broad band (which consists of two overlapping bands) around 1927 cm^{-1} for the former and 1921 cm^{-1} for the latter. No significant differences in CO stretching frequencies were observed between monometallic and bimetallic complexes.

X-ray Structure. An ORTEP[23] drawing of the $[Re(pypm\text{-}py)(py)(CO)_3]^+$ is shown in Figure 2. Selected bond distances and angles are given in Table 2. The $[Re(pypm\text{-}py)(py)(CO)_3]^+$ cation is found on a general position in the monoclinic space group $P2_1/n$. The asymmetric unit is completed by one trifluoromethanesulfonate counterion and one water molecule.

The coordination geometry around the Re center is *facial* with three carbonyl groups and three nitrogen imine donors. The three Re−C bond distances are ∼1.90 Å, whereas the Re−N bond distances vary. Two were similar: 2.202(9) Å to the nitrogen of the pyrimidine ring and 2.203(9) Å to the nitrogen of coordinated pyridine. The Re−N distance to the diimine nitrogen of the pyridine ring was shorter, 2.167(9) Å giving rise to a bite angle of 75.3° for N(1)−Re(1)−N(3). The pyridine ring was nearly opposite the carbonyl group as noted by the N(5)−Re(1)−C(22) angle of 177.3°, and the coordinated pyridine was slightly canted toward the pypm-py unit as indicated by the N(1)−Re(1)−N(5) angle of 85.3(3)° and the N(3)−Re(1)−N(5) angle of 84.4(3)°. The pypm portion of the pypm-py ligand was distorted with a dihedral angle of 8.26° between the coordinated py and pm rings. The dihedral angles between coordinated pyridine ring and the py and pm rings of coordinated pypm-py were 97.38° and 90.97°, respectively. The other dihedral angles of interest were between the uncoordinated pyridine ring attached to pypm and the pypm planes. The angles were 41.99° and 34.81° between it and the py and pm planes, respectively.

A comparison of the structure of $[Re(pypm\text{-}py)(py)(CO)_3]^+$ can be made to several related ones[10a,13e,24] where the Re−N(diimine) bond distances are found to vary. $[Re(bpm)(MeQ)(CO)_3]^{2+}$, where MeQ^+ is *N*-methyl-4,4′-bipyridinium ion and bpm is 2,2′-bipyrimidine, gave Re−N bond lengths of 2.180 (8) Å and 2.161(7) Å.[24a,b] Two sets of bond distances were found for $[Re(bpm)(CH_3CN)(CO)_3]^+$ since there were two independent cations per unit cell. The Re−N bond distances found were 2.198(10) and 2.187(12) Å to one diimine N and 2.171(9) and 2.161(12) Å to the other. The bond distance to the pyridine residue of the MeQ^+ ligand was 2.210(8) Å. Re−N bond distances in related diimine complexes containing 2,2′-bipyridine[10a,13e,24c−e,g] or 1,10-phenanthroline[24f] also revealed bond distance differences of Re to the diimine ligand. Typical Re−N bond distances ranged from 2.16 to 2.18 Å, but bond distances as short[24g] as 2.11 Å and as long[13e] as 2.24 Å were reported. Apparently, structure variations giving rise to differing Re−N bond distances in diimine complexes are normal for *facial* rhenium(I) complexes.

Electrochemistry. Cyclic voltammetric data for the complexes are collected in Table 3, which also contains comparable

(23) Johnson, C. K. ORTEP−A Fortran Thermal Ellipsoid Plot Program. Technical Report ORNL-5138; Oak Ridge National Laboratory: Oak Ridge, TN, 1976.

(24) (a) Winslow, L. N.; Rillema, D. P.; Welch, J. H.; Singh, P. *Inorg. Chem.* **1989**, *28*, 1596. (b) Shaver, R. J.; Perkovic, M. W.; Rillema, D. P.; Woods, C. *Inorg. Chem.* **1995**, *34*, 5446. (c) Strouse, G. F.; Gudel, H. U.; Bertolasi, V.; Ferretti, V. *Inorg. Chem.* **1995**, *34*, 5578. (d) Guilhem, J.; Pascard, C.; Lehn, J.-M.; Ziessel, R. *J. Chem. Soc., Dalton Trans.* **1989**, 1449. (e) Lin, J. T.; Sun, S.-S.; Wu, J. J.; Liaw, Y.-C.; Lin, K.-J. *J. Organomet. Chem.* **1996**, *517*, 217. (f) Wallace, L.; Woods, C.; Rillema, D. P. *Inorg. Chem.* **1995**, *34*, 2875. (g) Chen, P.; Curry, M.; Meyer, T. J. *Inorg. Chem.* **1989**, *28*, 2271.

Scheme 2. Synthetic Routes for Preparing Mono- and Bimetallic Complexes

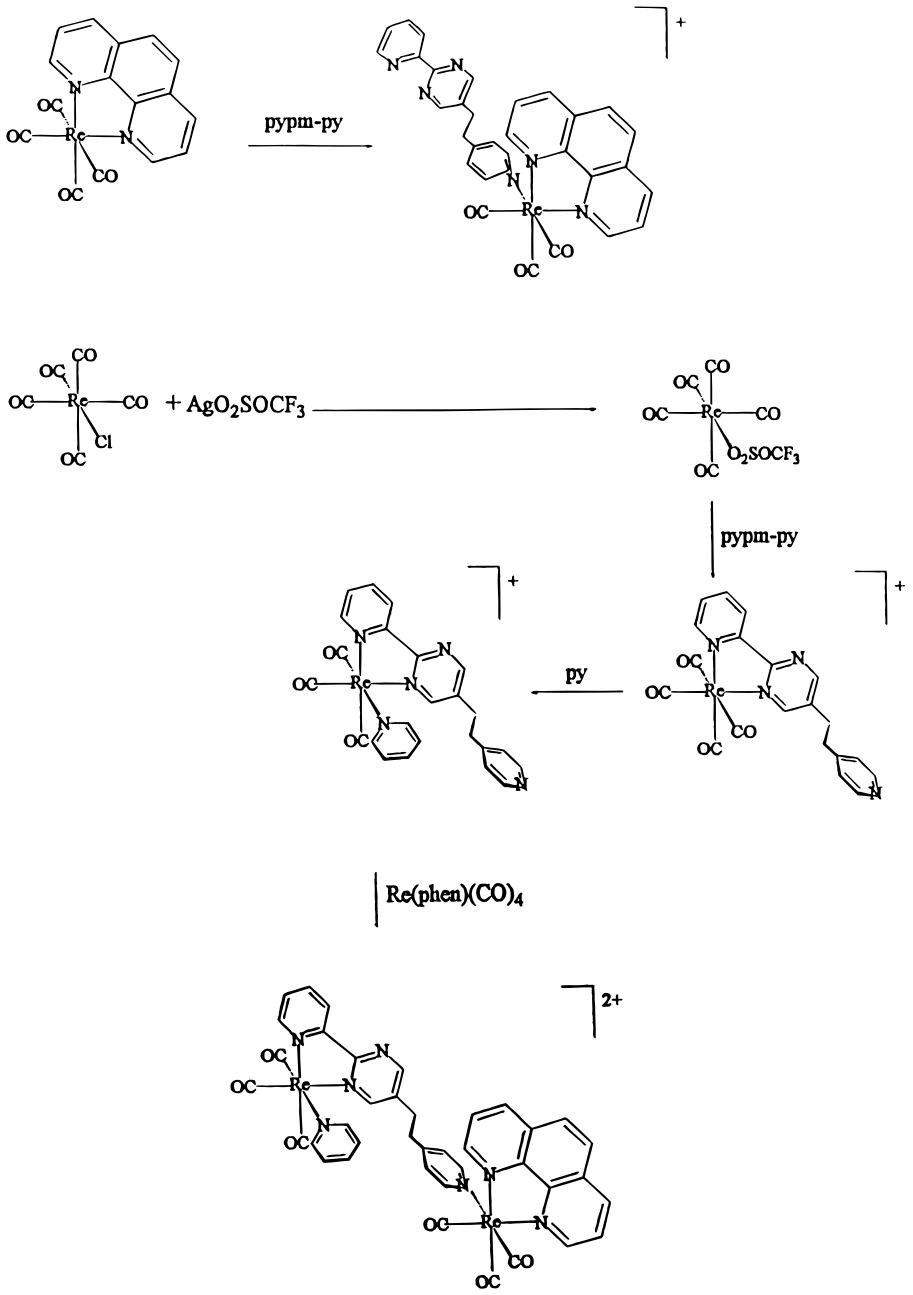

data for $[Re(phen)(py)(CO)_3]^+$. Each of the complexes studied here displayed an irreversible oxidation between +1.83 and +1.87 V vs SSCE and a series of three or four reductions in the −1.04 to −1.74 V range. On the basis of previous literature reports, the oxidation wave can be assigned to the metal-centered redox process, $Re^{2+/+}$, and the first reduction can be attributed to the reduction of the coordinated diimine ligands.[3c,10c,14a,25] The reduction potentials of the $Re^{2+/+}$ couples are almost identical for these three complexes but somewhat different from that for analogous $[Re(phen)(py)(CO)_3]^+$ which occurred at +1.69 V. This may be due to the chemically irreversible nature of these potentials.

The first reduction of $[Re(phen)(py\text{-}pypm)(CO)_3]^+$ at −1.23 V is attributed to reduction of coordinated 1,10-phenanthroline, $[Re(phen^{0/-})(py\text{-}pypm)(CO)_3]^{+/0}$. This potential is comparable to −1.22 V found for $[Re(phen)(py)(CO)_3]^+$. The first reduction of $[Re(pypm\text{-}py)(py)(CO)_3]^+$ at −1.04 V and of bimetallic compound $[(CO)_3(py)Re(pypm\text{-}py)Re(phen)(CO)_3]^{2+}$ at −1.06 V is assigned to the reduction of coordinated pypm-py$^{0/-}$, $[Re(pypm\text{-}py)^{0/-}(py)(CO)_3]^{+/0}$. This potential falls midway between ones reported for $[Ru(bpm)(py)(CO)_3]^{+/0}$ assigned to reduction of the bpm ligand[24b] and the analogues containing phen[14a] or bpy[24c,26] ligands. This is expected based on the concepts of Lever[27] where the types of ligands can be used to predict redox potentials coordinated to metal centers based on their redox potentials in analogous complexes.

Electronic Absorption Spectra. Absorption spectra for the complexes were obtained in acetonitrile, 4:1 ethanol/methanol, and 1,2-dichloroethane, and the results are presented in Table

(25) (a) Lin, R.; Guarr, T. F. *Inorg. Chim. Acta* **1990**, *167*, 149. (b) Taposky, G.; Duesing, R.; Meyer, T. J. *Inorg. Chem.* **1990**, *29*, 2285. (c) Caspar, J. V.; Meyer, T. J. *J. Phys. Chem.* **1983**, *87*, 952. (d) Luong, J. C.; Nadjo, L.; Wrighton, M. S. *J. Am. Chem. Soc.* **1978**, *100*, 5790.

(26) Lucia, L. A.; Abboud, K.; Schanze, K. *Inorg. Chem.* **1997**, *36*, 6224.

(27) Lever, A. B. P. *Inorg. Chem.* **1990**, *29*, 1271.

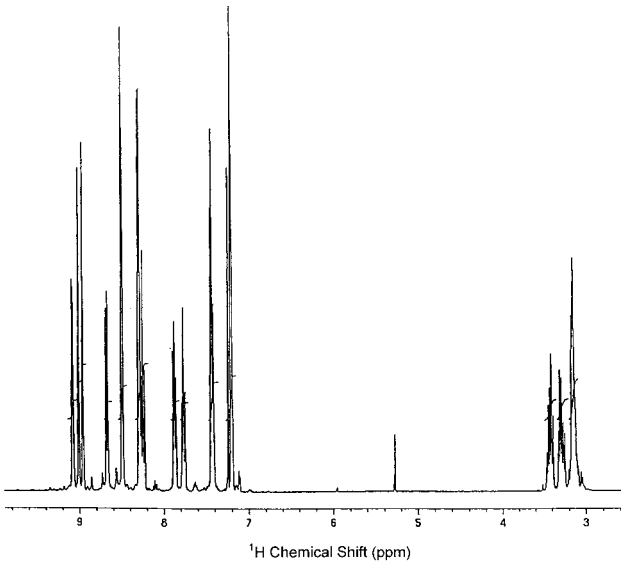

Figure 1. ^{1}H NMR spectrum ($CDCl_3$, 400 MHz) of [Re(pypm-py)(py)$(CO)_3]^+$.

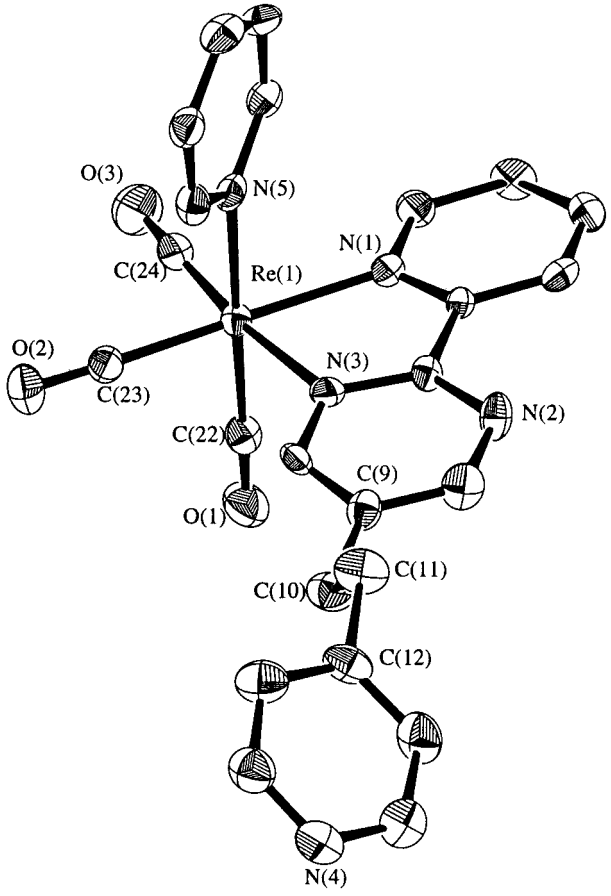

Figure 2. ORTEP drawing of the [Re(pypm-py)(py)$(CO)_3]^+$ cation. Ellipsoids are drawn at the 50% probability level, and hydrogen atoms have been omitted for clarity.

4. The spectra of the monometallic and bimetallic complexes studied here are very similar to those reported for analogous Re(I) diimine complexes.[3c,4c,d,10c,25c,d] One key feature of these spectra is the appearance of a very broad, moderately intense band in the 320−430 nm region, which has been attributed to a metal-to-ligand charge transfer absorption. According to electrochemical data and their assignments, the lowest energy absorptions for [Re(pypm-py)(py)$(CO)_3]^+$, [Re(phen)(py-pypm)$(CO)_3]^+$, and [$(CO)_3$(py)Re(pypm-py)Re(phen)$(CO)_3]^{2+}$ are attributed to dπ(Re) → π^*(pypm-py), dπ(Re) → π^*(phen), and dπ(Re) → π^*(pypm-py), respectively. Owing to their broad absorption manifolds, there is little observable difference in maxima of the lowest energy absorptions. The electronic spectrum of the bimetallic compound exhibits the same characteristic shape as that of the monometallic complexes, but the molar absorptivity of the lowest energy absorption is significantly larger (roughly a factor of 2). The lowest absorption band of the bimetallic complex is most likely due to overlapping MLCT transitions directed to the pypm-py and phen ligands accounting for the increased absorption coefficient. The differences in the reduction potentials are not enough to allow for an unequivocal assignment of the MLCT transition.

Table 2. Selected Bond Lengths and Angles

Bond lengths, Å			
Re(1)−N(1)	2.167(9)	Re(1)−C(24)	1.89(2)
Re(1)−N(5)	2.203(9)	C(10)−C(11)	1.54(2)
Re(1)−C(23)	1.90(1)	C(9)−C(10)	1.51(2)
Re(1)−N(3)	2.202(9)	C(11)−C(12)	1.49(2)
Re(1)−C(22)	1.91(1)	C(23)−O(2)	1.16(1)
Bond angles, deg			
N(1)−Re(1)−N(3)	75.3(3)	N(5)−Re(1)−C(24)	96.0(4)
N(1)−Re(1)−C(24)	96.4(4)	N(5)−Re(1)−C(22)	177.3(4)
N(1)−Re(1)−N(5)	85.3(3)	N(5)−Re(1)−C(23)	91.4(4)
N(1)−Re(1)−C(23)	173.7(4)	C(22)−Re(1)−C(24)	86.7(5)
N(1)−Re(1)−C(22)	94.6(4)	C(22)−Re(1)−C(23)	88.4(5)
N(3)−Re(1)−N(5)	84.4(3)	C(23)−Re(1)−C(24)	89.2(5)
N(3)−Re(1)−C(22)	93.0(4)	C(10)−C(11)−C(12)	110(1)
N(3)−Re(1)−C(23)	99.1(4)	C(9)−C(10)−C(11)	112(1)
N(3)−Re(1)−C(24)	171.7(4)		

Photophysical Properties. All of the complexes studied here displayed strong luminescence both in room temperature fluid solution and in the glassy state at 77 K (Table 5). The emission spectra at room temperature were broad. The glassy state emission spectra in 4:1 ethanol/methanol at 77 K were also broad and structureless, but the emission maxima were shifted to higher energy. The emission spectral profiles and excited-state lifetimes at room temperature and at 77 K were excitation wavelength independent, and the emission quantum yields were also constant using 300−400 nm excitation. Emission spectra profiles at room temperature and at 77 K were typical of ^{3}MLCT emitters.

The emission maxima of [Re(pypm-py)(py)$(CO)_3]^+$ were located at the same position, ca. 570 nm in 4:1 ethanol/methanol and in acetonitrile, but blue shifted to 552 nm in dichloroethane. The quantum yields were nearly constant in 4:1 ethanol/methanol (0.014) and acetonitrile (0.020) but increased to 0.074 in dichloroethane. The emission lifetimes followed the same trends: 0.11 μs in ethanol/methanol, 0.15 μs in acetonitrile, but 0.42 μs in dichloroethane. The excited state is assigned to ^{3}[dπ(Re) → π^*(pypm-py)].

The luminescence behavior of [Re(phen)(py-pypm)$(CO)_3]^+$ is also solvent dependent but different from that of [Re(pypm-py)(py)$(CO)_3]^+$. Although the polarity of acetonitrile and dichloroethane differs greatly, the emission energy (534 nm in acetonitrile and 532 nm in dichloroethane), quantum yields (0.47 in acetonitrile and 0.45 nm in dichloroethane), and emission lifetimes (3.27 μs in acetonitrile and 3.18 μs in dichloroethane) were almost constant. However, in ethanol/methanol at room temperature, the emission is red shifted to 548 nm with a lower quantum yield of 0.087 and a shorter lifetime of 1.65 μs. This behavior is different from analogous [Re(phen)(py)$(CO)_3]^+$ where the emission maximum shifts from 544 nm in CH_2Cl_2 to

Table 3. Electrochemical Data[a]

complex	oxidation	reduction			
$[Re(pypm\text{-}py)(py)(CO)_3]^+$	+1.85 (irr)	−1.04 (80)	−1.40 (114)	−1.64 (126)	
$[Re(phen)(py\text{-}pypm)(CO)_3]^+$	+1.83 (irr)	−1.23 (irr)	−1.39 (irr)	−1.61 (irr)	
$[(CO)_3(py)Re(pypm\text{-}py)Re(phen)(CO)_3]^{2+}$	+1.87 (irr)	−1.06 (irr)	−1.15 (irr)	−1.61 (irr)	−1.74 (irr)
$[Re(phen)(py)(CO)_3]^+$ [b]	+1.69 (200)	−1.22 (irr)	−1.66 (70)	−1.82 (95)	

[a] All potentials are vs SSCE, scan rate is 100 mV/s, error is ±0.02 V, ΔE_p in parentheses for reversible peaks. [b] From the data in ref 14a.

Table 4. UV−Visible Spectral Data

complex	medium[a]	d → π*, nm (ε, M^{-1} cm^{-1})	π → π*, nm (ε, M^{-1} cm^{-1})
$[Re(pypm\text{-}py)(py)(CO)_3]^+$	E-M	340 (br, 6.80×10^3)	258 (3.17×10^4), 284 (2.68×10^4), 304 (sh, 1.76×10^4)
	MeCN	350 (br, 5.12×10^3)	256 (2.72×10^4), 282 (2.34×10^4), 308 (sh, 1.28×10^4)
	DCE	340 (br, 5.45×10^3)	276 (sh, 3.27×10^4), 304 (sh, 1.71×10^4)
$[Re(phen)(py\text{-}pypm)(CO)_3]^+$	E-M	340 (br, 5.92×10^3)	250 (3.76×10^4), 266 (3.89×10^4), 288 (sh, 2.66×10^4)
	MeCN	350 (br, 4.64×10^3)	248 (3.58×10^4), 274 (3.91×10^4), 320 (sh, 7.6×10^3)
	DCE	340 (br, 5.90×10^3)	276 (4.73×10^4)
$[(CO)_3(py)Re(pypm\text{-}py)Re(phen)(CO)_3]^{2+}$	E-M	340 (br, 1.44×10^4)	256 (br, 5.54×10^4)
	MeCN	350 (br, 1.17×10^4)	258 (4.79×10^4), 274 (4.88×10^4), 304 (2.84×10^4)
	DCE	340 (br, 1.27×10^4)	272 (8.17×10^4), 294 (sh, 4.46×10^4)
$[Re(phen)(py)(CO)_3]^+$ [b]	CH_2Cl_2	384 (3.6×10^3)	234 (2.2×10^4), 263 (2.8×10^4), 278 (2.4×10^4)

[a] E-M is 4:1 (v:v) ethanol/methanol, MeCN is acetonitrile, DCE is 1,2-dichloroethane. [b] From the data in ref 14a.

Table 5. Excited-State Properties

complex	medium[a]	λ_{em}/max, nm[c]	ϕ_{em}	τ, μs[d]	k_r, s^{-1}	k_{nr}, s^{-1}
$[Re(pypm\text{-}py)(py)(CO)_3]^+$	E-M, 77 K	505		4.75		
	E-M, 293 K	569	0.014	0.11	1.27×10^5	8.96×10^6
	MeCN, 293 K	570	0.020	0.15	1.33×10^5	6.53×10^6
	DCE, 293 K	552	0.074	0.42	1.76×10^5	2.20×10^6
$[Re(phen)(py\text{-}pypm)(CO)_3]^+$	E-M, 77 K	507		14.5		
	E-M, 293 K	548	0.087	1.65	5.27×10^4	5.53×10^5
	MeCN, 293 K	534	0.47	3.27	1.44×10^5	1.62×10^5
	DCE, 293 K	532	0.45	3.18	1.42×10^5	1.72×10^5
$[(CO)_3(py)Re(pypm\text{-}py)Re(phen)(CO)_3]^{2+}$	E-M, 77 K	503		9.57		
	E-M, 293 K	550	0.037	1.09	3.39×10^4	8.84×10^5
	MeCN, 293 K	549	0.065	1.61	4.04×10^4	5.81×10^5
	DCE, 293 K	542	0.072	1.16	6.21×10^4	8.00×10^5
$[Re(phen)(py)(CO)_3]^+$ [b]	E-M, 77 K	474, 497		11.7 ± 1.3		
	MeCN, 293 K	567	0.18	1.6		
	CH_2Cl_2, 293 K	544		3.0		

[a] E-M is 4:1 (v:v) ethanol/methanol, MeCN is acetonitrile, DCE is 1,2-dichloroethane. [b] From the data in ref 14a. [c] λ_{ex} = 355 nm, error ±2 nm. [d] Error ±10%.

567 nm in acetonitrile, and its emission lifetime decreased from 3.0 μs in CH_2Cl_2 to 1.6 μs in more polar acetonitrile.[14a] The excited state of $[Re(phen)(py\text{-}pypm)(CO)_3]^+$ is dominated by the $^3[d\pi(Re) \rightarrow \pi^*(phen)]$ transition both at room temperature and at 77 K, but the py-pypm ligand plays a role in altering the photophysical properties compared to the py ligand.

The luminescence behavior of bimetallic compound $[(CO)_3(py)Re(pypm\text{-}py)Re(phen)(CO)_3]^{2+}$ is similar to that of $[Re(pypm\text{-}py)(py)(CO)_3]^+$. The emission energy remained constant at ca. 550 nm in ethanol/methanol and acetonitrile but blue shifted to 542 nm in dichloroethane. Comparing the data in Table 5 and Figure 3, we find that the emission energies, quantum yields, and excited-state lifetimes of the bimetallic compound differed from those of the corresponding monometallic species. The excited-state data of the dimer is located between those of the monomers. The emission energy of $[(CO)_3(py)Re(pypm\text{-}py)Re(phen)(CO)_3]^{2+}$ is higher than that of $[Re(pypm\text{-}py)(py)\text{-}(CO)_3]^+$ but lower than that of $[Re(phen)(py\text{-}pypm)(CO)_3]^+$; quantum yields and lifetimes follow the same trends. Although the emission of $[(CO)_3(py)Re(pypm\text{-}py)Re(phen)(CO)_3]^{2+}$ is considered to come from $^3[d(Re) \rightarrow \pi^*(pypm\text{-}py)]$, there is obviously an interaction between the two rhenium atoms through the pypm-py bridging ligand. As described above, absorption of light in the MLCT region resulted in formation of both Ru(phen)* and Ru(pypm-py)*, but it is unlikely that both events occur within the same molecule. Thus, energy transfer occurs from Ru(phen)* to Ru(pypm-py), resulting in an increased quantum efficiency of the dimer compared to $[Re(pypm\text{-}py)(py)\text{-}(CO)_3]^+$. This is reasonable given the lower energy π^* level of pypm-py compared to phen as noted by the reduction potentials of the coordinated ligands.

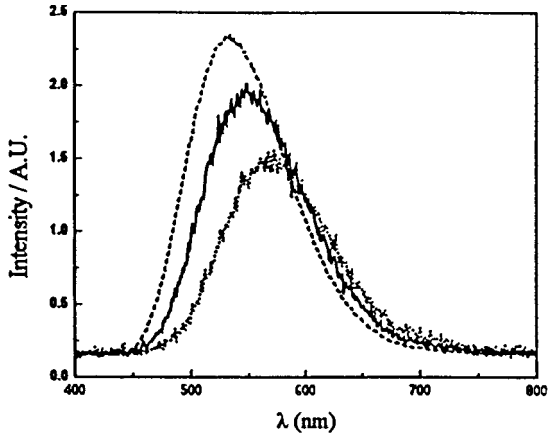

Figure 3. Emission spectra of $[Re(pypm\text{-}py)(py)(CO)_3]^+$ (···), $[Re(phen)(py\text{-}pypm)(CO)_3]^+$ (- - -), and $[(CO)_3(py)Re(pypm\text{-}py)Re(phen)\text{-}(CO)_3]^{2+}$ (—) in acetonitrile at room temperature.

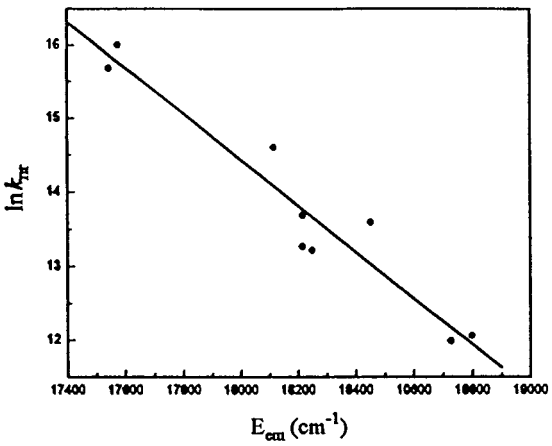

Figure 4. Plot of ln k_{nr} vs E_{em}.

An analysis of the nonradiative decay rates for the complexes in different solvents showed that the nonradiative decay rate constants increased when the excited-state energies decreased. A linear relationship of ln k_{nr} vs E_{em} with a correction of -0.96 is observed and presented in Figure 4. This effect can be understood in terms of the energy gap law. The quantitative application of the energy gap law has been presented by Meyer et al. and others for (i) complexes of the type $M(NN)_n(LL)_{3-n}^{2+}$ ($M = Os, Ru$; $n = 1, 2$),[28] where NN represents a diimine ligand and LL represents a different diimine ligand or a nonchromophoric ligand, and $Re(bpy)(CO)_3L^{+}$,[28a] where the energy gap was tuned by variation in the nonchromophoric ligand L, Re^{V} benzylidyne complexes containing phosphine ligands,[29] (ii) complexes of the type $Os(NN)_n(LL)_{3-n}^{2+}$ ($n = 0-3$),[30] $Ru(NN)_3^{2+}$,[31] and Pt(NN)(tdt),[32] where tdt is a dithiolate ligand and the energy gap was tuned by the variation in the chromophoric diimine ligand NN, (iii) $Ru(bpy)_3^{2+}$,[33] and Pt(5-ph-phen)$(CN)_2$,[34] where 5-ph-phen is 5-phenyl-1,10-phenanthroline and the energy gap was tuned by variation in the solvent, and (iv) $Os(phen)_3^{2+}$,[3a] for which the energy gap was tuned by variation in the counterion.

In summary, one of the goals of the project was to examine the effect of energy transfer from an attached complex with a higher energy excited state than the complex responsible for emission. In the dimer $[(CO)_3(py)Re(pypm\text{-}py)Re(phen)(CO)_3]^{2+}$, the data clearly indicate that emission occurs via the "$(CO)_3(py)Re(pypm\text{-}py)$" unit based on quantum efficiencies tabulated in Table 5. The quantum efficiencies in 4:1 ethanol/methanol and acetonitrile are clearly increased by factors up to 3 compared to $[(CO)_3(py)Re(pypm\text{-}py)]^{+}$. The absorption coefficients in the region of excitation indicate that both rhenium chromophores absorb with approximately the same efficiency. Thus, energy transfer from the lowest lying excited state of "$(pypm\text{-}py)Re(phen)(CO)_3^{+}$*" to the lowest lying excited state of "$(CO)_3(py)Re(pypm\text{-}py)^{+}$*" would account for the enhanced emission quantum yields in the dimer, since nonradiative decay from the singlet state to the ground state in "$(CO)_3(py)Re(pypm\text{-}py)^{+}$" would be avoided. The observations found here were similar to those reported earlier for a mixed−metal complex, Re−L−Ru, where the quantum efficiency for emission from the lowest excited state, in this case Ru, was increased by energy transfer from the Re chromophore to the Ru unit.

Acknowledgment. We thank the Office of Basic Energy Sciences of the United States Department of Energy for support of the investigation and the National Science Foundation for the 400 MHz NMR and the laser equipment.

Supporting Information Available: Tables listing detailed crystallographic data, atomic positional parameters, and bond lengths and angles. Figure of the UV/visible absorption spectra of $[Re(pypm\text{-}py)(py)(CO)_3]^{+}$, $[Re(phen)(py\text{-}pypm)(CO)_3]^{+}$, and $[(CO)_3(py)Re(pypm\text{-}py)Re(phen)(CO)_3]^{2+}$ in acetonitrile. This material is available free of charge via the Internet at http://pubs.acs.org.

IC000134D

(28) (a) Caspar, J. V.; Meyer, T. J. *Inorg. Chem.* **1983**, *22*, 2444. (b) Caspar, J. V.; Kober, E. M.; Sullivan, B. P.; Meyer, T. J. *J. Am. Chem. Soc.* **1982**, *104*, 630. (c) Kober, E. M.; Caspar, J. V.; Lumpkin, R. S.; Meyer, T. J. *J. Phys. Chem.* **1986**, *90*, 3722. (d) Kober, E. M.; Marshall, J. L.; Dressick, W. J.; Sullivan, B. P.; Caspar, J. V.; Meyer, T. J. *Inorg. Chem.* **1985**, *24*, 2155. (e) Kalyanasundaram, K.; Nazeeruddin, M. K. *Chem. Phys. Lett.* **1992**, *193*, 292.

(29) Xue, W. M.; Wang, Y.; Mak, T. C. W.; Che, C. M. *J. Chem. Soc., Dalton Trans.* **1996**, 827.

(30) Johnson, S. R.; Westmoreland, T. D.; Caspar, J. V.; Barqawi, K. R.; Meyer, T. J. *Inorg. Chem.* **1988**, *27*, 3195.

(31) Cook, M. J.; Lewis, A. P.; McAuliffe, G. S. G.; Skarda, V.; Thomson, A. J.; Glasper, J. L.; Robbins, D. J. *J. Chem. Soc., Perkin Trans. 2* **1984**, 1293.

(32) Cummings, S. D.; Eisenberg, R. *J. Am. Chem. Soc.* **1996**, *118*, 1949.

(33) Caspar, J. V.; Meyer, T. J. *J. Am. Chem. Soc.* **1983**, *105*, 5583.

(34) Chan, C. W.; Cheng, L. K.; Che, C. M. *Coord. Chem. Rev.* **1994**, *132*, 87.